AIP Applied Physics Letters

Geometrical correlations of quantum dots in InAs/GaAs superlattice structure from electron tomography

Y. H. Wu, L. Chang, L. C. Chen, H. S. Chen, and F. R. Chen

Citation: Applied Physics Letters **93**, 153108 (2008); doi: 10.1063/1.2998693
View online: http://dx.doi.org/10.1063/1.2998693
View Table of Contents: http://scitation.aip.org/content/aip/journal/apl/93/15?ver=pdfcov
Published by the AIP Publishing

Articles you may be interested in

Site-controlled formation of InAs/GaAs quantum-dot-in-nanowires for single photon emitters
Appl. Phys. Lett. **100**, 263101 (2012); 10.1063/1.4731208

Influence of wetting layers and quantum dot size distribution on intermediate band formation in InAs/GaAs superlattices
J. Appl. Phys. **110**, 073105 (2011); 10.1063/1.3631785

Characterization of excitonic features in self-assembled InAs/GaAs quantum dot superlattice structures via surface photovoltage spectroscopy
J. Appl. Phys. **101**, 103102 (2007); 10.1063/1.2733992

Mechanisms of lateral ordering of InAs/GaAs quantum dot superlattices
J. Vac. Sci. Technol. B **21**, 1920 (2003); 10.1116/1.1588645

Structural characterization of InAs/GaAs quantum-dot nanostructures
Appl. Phys. Lett. **78**, 4133 (2001); 10.1063/1.1382855

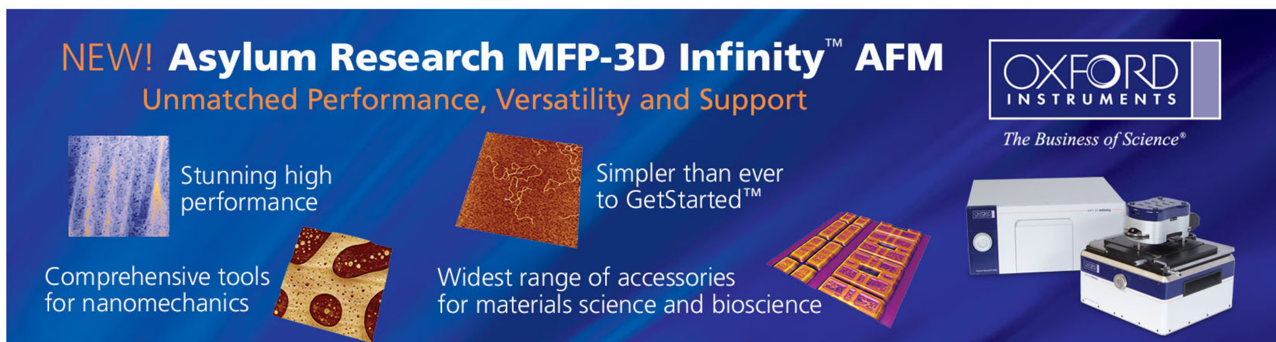

This article is copyrighted as indicated in the article. Reuse of AIP content is subject to the terms at: http://scitation.aip.org/termsconditions. Downloaded to IP: 140.113.38.11 On: Wed, 30 Apr 2014 22:52:18

Geometrical correlations of quantum dots in InAs/GaAs superlattice structure from electron tomography

Y. H. Wu,[1,a] L. Chang,[1] L. C. Chen,[2] H. S. Chen,[3] and F. R. Chen[3]
[1]*Department of Materials Science and Engineering, National Chiao-Tung University, Hsinchu 300, Taiwan*
[2]*Process Failure Analysis Department, Taiwan Semiconductor Manufacturing Company Ltd., Science-Based Industrial Park, Hsinchu 300, Taiwan*
[3]*Department of Engineering and System Science, National Tsing-Hua University, Hsinchu 300, Taiwan*

(Received 7 May 2008; accepted 22 September 2008; published online 14 October 2008)

In this study, the three-dimensional (3D) information about the structural properties of quantum dots (QDs) in InAs/GaAs superlattice structure has been illustrated using electron tomography in the mode of high-angle angular dark-field scanning transmission electron microscopy. Comparison of this 3D reconstruction with the two-dimensional projection at the same positions is made. The structural properties of embedded quantum dots have been evaluated from electron tomography. The correlation relationship of QDs in superlattice structure has been understood by accurate measurements of 3D geometric positions, which can be free of the overlapping effect from 2D cross section along different crystallographic orientations. © *2008 American Institute of Physics*.
[DOI: 10.1063/1.2998693]

Self-assembled semiconductor quantum dots (QDs) formed by the Stranski–Krastanow growth mode due to lattice mismatch are valuable nanostructures because of their outstanding electronic and optical properties, especially for laser applications.[1,2] Varying depositing conditions of QDs may modify the structural properties due to the strain field around QDs, such as size, shape, and density, that strongly influence electronic structure of nanostructures and the band gap.[3] However, luminescence intensity of QDs in a single layer cannot meet the requirement for laser applications. For practical usage, semiconductor QDs are normally grown in superlattice structures in order to improve the luminescence yield, so characteristic arrangements of QDs could be resulted from the interaction between vertical and lateral strain fields among different layers.[4–6] The periodic features in the superlattice quantum structure depending on the spacer thickness may have either correlated or anticorrelated arrangement. The phenomena had been reported in the heterostructure superlattice systems such as InAs/GaAs, InAs/InP, PbSe/PbEuTe, CdSe/ZnSe, and SiGe/Si.[7–10] Scanning tunneling microscopy (STM) and transmission electron microscopy (TEM) in cross section are often the main tools to characterize the structural properties of embedded QDs, which only reveal two-dimensional (2D) information.[11,12] TEM observations of correlated QDs in superlattice structures using projected data may not easily uncover the real structure due to the overlapping effect in 2D, as a result of lacking third dimension information. In addition, for conventional TEM in bright-field and dark-field images, the strain-induced diffraction contrast may shed the QDs in a 100–200 nm thick TEM specimen. High-resolution transmission electron microscopy (HRTEM) observations of some characteristic properties of QDs such as size and shape are a difficult task because a thin sample of thickness less than 20–40 nm for requirements of HRTEM may lack sufficient number of QDs. Incomplete STM data in the depth direction may show uncertainty for buried QDs as well.

TEM electron tomography has been well established for three-dimensional (3D) characterization of biological and amorphous materials.[13,14] Although the electron tomography using bright-field TEM and energy-filtered TEM can be achieved in principle for crystalline materials, they may not be easy to obtain the acceptable 3D information because of the diffraction contrast effect, limitation of specimen thickness, and poor signal-to-noise ratio.[15] Electron tomography reconstructed from a tilt series of high-angle angular dark-field scanning transmission electron microscopy (HAADF-STEM) images is a promising technique for the investigation of crystalline materials in 3D.[16] The contrast in HAADF-STEM images is approximately proportional to $Z^{1.7}$ (Z is the atomic number of the scattering atom), which can be interpreted in terms of the relative element ratio directly.[17] Arslan *et al.*[18] used the HAADF-STEM imaging technique to demonstrate electron tomography for nanocrystals and Ge/Si QDs. More recently, Inoue *et al.*[19] demonstrated HAADF-STEM electron tomography for a single embedded InAs QD in GaAs. The only study of tomography of QD superlattice has been recently done by Müller *et al.*[20] using 3D atom probe technique. Here, we investigated 3D geometrical correlations of capped QDs in InAs/GaAs superlattice structure using electron tomography based on HAADF-STEM mode from which 3D crystallographic information can be extracted.

The self-assembled QDs superlattice structure on GaAs (001) substrates consisted of 30 periods of InAs (2.62 monolayers) and GaAs spacer layer (30 nm), which were grown by molecular beam epitaxy at 485 and 600 °C, respectively. For [010] cross-sectional TEM specimen preparation, mechanical grinding and polishing were used to thin a specimen to about 500 nm thickness, followed by Ar^+ milling at 4 kV with a low incident angle. The 5 nm colloidal gold particles in acetone were dropped uniformly onto a TEM specimen as fiducial markers for accurate alignment of acquisition of a tilt series of HAADF-STEM images and for reconstruction. In this study, electron tomography was performed in a FEI Tecnai F20 microscope with a high-tilt single-axis sample holder. STEM-HAADF images were acquired on a Fischione

[a]Electronic mail: yhwu.mse91g@nctu.edu.tw.

 © 2008 American Institute of Physics

This article is copyrighted as indicated in the article. Reuse of AIP content is subject to the terms at: http://scitation.aip.org/termsconditions. Downloaded to IP: 140.113.38.11 On: Wed, 30 Apr 2014 22:52:18

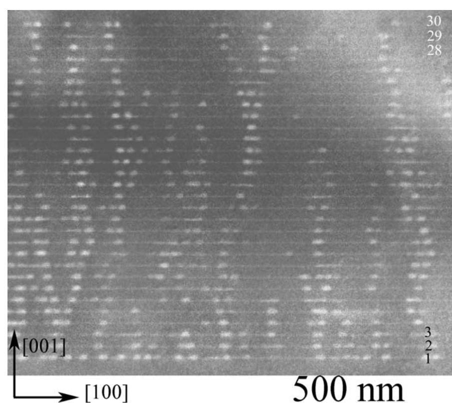

FIG. 1. Cross-sectional HAADF-STEM image showing QDs InAs/GaAs superlattice structure in [010].

Model 3000 annular dark field detector with an inner collection angle about 70 mrad at a magnification of 225 000× using a 1 nm probe. The FEI XPlore 3D tomography suite was used to control the operation of image acquisition in a wide range of tilt angle from −70° to +70° in 1° increments with the tilt axis along $[001]_{GaAs}$ to minimize the missing wedge effect. After complete alignment of TEM, automatic operation of recentering and refocusing STEM-HAADF images of gold particles by the phase-correlation method was adopted during this tilting process.[21] The weighted back-projected algorithm used for reconstruction of tomography data from the 141 tilt-series images was performed with the FEI program. The GaAs spacer layer thickness in such a superlattice structure can be used for z-axis scale calibration. The successfully reconstructed data did display a rotational movie smoothly without any jumpiness. Furthermore, the wedge shape of the TEM specimen was faithfully exhibited in reconstructed tomography.

Figure 1 shows a HAADF image of the whole QD superlattice structure taken along GaAs [010] direction at low magnification. The bright regions are indium-rich and correspond to the wetting layers and QDs. It is seen the 30 periods of alternating InAs QDs and wetting layers with 30 nm GaAs spacer. The wetting layer as a set of white parallel lines is about 1 nm thick with the indium concentration of $x \sim 0.12$ in $In_xGa_{1-x}As$ as determined from the Z-contrast values relative to the GaAs ones. Observations of vertical arrangement of InAs QDs in this projected image show that the QDs are distributed in an angular range of 65°–85° with respect to the wetting layer surface, indicating that the QDs may not be vertically aligned.

The tomographic reconstruction in Fig. 2(a) of a 3D perspective view shows the distribution of 72 QDs within the top eight layers of the whole structure in a rectangular parallel-piped volume of $133 \times 524 \times 240\ \text{nm}^3$. The inset in Fig. 2(a) shows two of the QDs in the 27th layer after volume rendering. For quantitative analysis of the superlattice structure, sliced images and segmentation of a reconstructed volume were used to examine the shape, the size, and distribution of the QDs. Typical sliced images from three adjacent layers (28th to 26th) are illustrated in Fig. 2(b). From the reconstruction, the shape of the buried QDs can be recognized as lenslike, and the size of the QDs within the eight layers is estimated to be around 18–25 nm in width as measured along [100] and [010] and about 7 nm above the wetting layers in height in the growth direction of [001]. It can

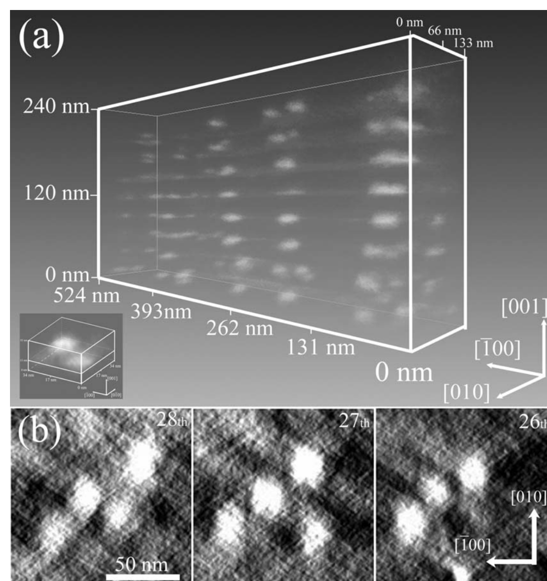

FIG. 2. (a) Volume rendering of reconstruction showing the distribution of InAs QDs within the top eight layers. The bright contrast obtained after removing GaAs background corresponds to indium-containing regions. The inset showing two of the QDs. (b) Typical sliced images from three adjacent layers (layers 28–26).

also be shown that the size of the QDs is not uniformly distributed. The density of QDs in each layer is determined from the sliced images of the total eight layers (not shown). Since the volume contains only 72 QDs in this tomography data set, it may not give good statistics with accuracy. There is about 14% difference in the density of QDs in the same volume between the values determined from the 3D reconstruction and from the 2D projections due to the overlapping effect. The difference may increase significantly in the cases of a high QD density structure and a thicker TEM specimen with increased possibility of the overlap.

Figure 3(a) is a histogram from 45 pairs of QDs within the reconstructed volume, showing the distances of the first nearest neighbor (the 1st NN) of QDs in adjacent layers. The

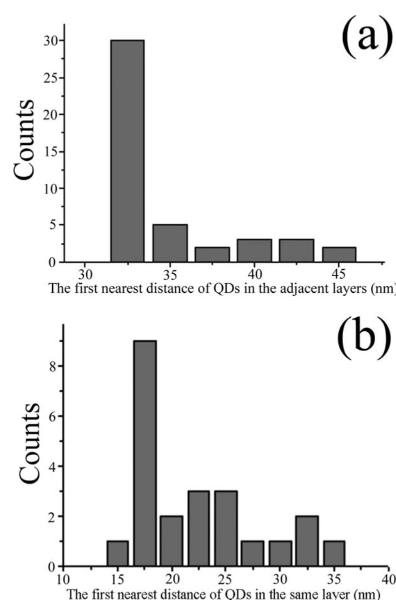

FIG. 3. (a) Histogram of the nearest neighboring distance between QDs in the adjacent layers. (b) Histogram of the nearest neighboring distance between QDs in the same layer.

This article is copyrighted as indicated in the article. Reuse of AIP content is subject to the terms at: http://scitation.aip.org/termsconditions. Downloaded to IP: 140.113.38.11 On: Wed, 30 Apr 2014 22:52:18

distances of the 1st NN measured from base-center to base-center of neighboring QDs are important for quantification of geometric correlations. Most of the distances are 32.5 nm, which is slightly larger than the periodic GaAs spacer thickness in 30 nm. This result suggests that the strain caused by the underlying QDs may laterally displace the lateral positions of subsequently formed QDs. Lateral shift of a deposited dot with respect to a buried one in an underlying layer is about 8.8 nm along ⟨110⟩ and the vertically deviated angle from [001] is about 15°. The histogram in Fig. 3(b) illustrates the distribution of the distance of the 1st NN of 23 pairs QDs in the same layer to show 2D arrangement of QDs, and most of the distances appear to be about 17.5 nm, which is equal to two times lateral shift in the adjacent layers.

Figure 4(a) is a projected view of a local volume [the same region to show the sliced images in Fig. 2(b)] along [100]. The included angle between lines $\overline{12}$ and $\overline{23}$ among the three dots denoted as 1, 2, and 3 in Fig. 4(a) of a 2D projection image is 72.8°. However, the real angle in 3D between these three QDs as measured from the sliced images of these two layers from the reconstructed tomography data is actually 82°. Detailed analysis of the QDs in the eight layers shows that the characteristic 3D angle is $80 \pm 5°$.

Furthermore, electron tomography provides observations of a crystalline specimen along various orientations. The projected images of the same QDs distributed in 3D can be visualized along [100], [$1\bar{1}0$], [110], and [001] crystallographic orientations as shown in Figs. 4(a)–4(d), respectively. Due to the relatively thick specimen and the tilting limit of the sample holder, it is almost impossible to observe structural properties of capped QDs in conventional TEM in such a wide range of projection directions. TEM evidence of GaAs-based nanostructures along [110] direction has been presented in many studies because of relatively easy specimen preparation and observation, but the symmetric properties of QDs may be sometimes lost from the data in a single crystallographic orientation. Projected images such as Figs. 4(a)–4(c) may not realize the real situation that QDs are aligned approximately along ±[$1\bar{1}0$] and ±[110] directions. From Figs. 4(a) and 4(c), the measured width of QDs in the [100] projected image is smaller than in the[110] one, implying that the base of QDs may be not circular. If we observe the QDs from [$00\bar{1}$], the shape of quantum dots is nearly like a rectangle as shown in Fig. 4(d), and the edges of the quantum dots are parallel to ⟨100⟩ in consistence with observations of planar QDs arrays in InAs/GaAs system in other studies.[19,22]

In summary, the actual behavior of capped quantum dots in InAs/GaAs superlattice structure with 30 nm thick GaAs spacer has been successfully revealed using electron tomography with the HAADF-STEM technique. The reconstruction shows that the shape of embedded InAs QDs is lenslike. Most of the embedded QDs in 3D distribution form a characteristic arrangement in the adjacent layers with lateral shift of 8.8 nm in ⟨110⟩ relative to the underlying QDs and an included angle of 80° among three neighboring QDs in adjacent layers.

The authors thank Taiwan Semiconductor Manufacturing Co. (TSMC) for supporting this research and providing the tomography facilities and Y. F. Kao for the help on STEM operation. The QD samples were provided by R. S. Hsiao of Industrial Technology Research Institute, Hsinchu, Taiwan.

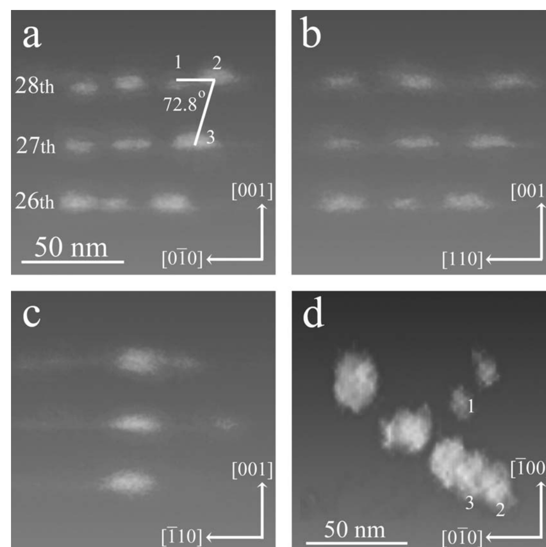

FIG. 4. Projections of QDs within a local volume from 26–28th layers along (a) [100], (b) [$1\bar{1}0$], (c) [110], and (d) [001] zone axes showing the relative geometric positions of InAs QDs in the adjacent layers.

[1] V. A. Shchukin and D. Bimberg, Rev. Mod. Phys. **71**, 1125 (1999).
[2] V. M. Ustinov and A. E. Zhukov, Semicond. Sci. Technol. **15**, R41 (2000).
[3] M. Grundmann, O. Stier, and D. Bimberg, Phys. Rev. B **52**, 11969 (1995).
[4] A. E. Zhukov, A. R. Kovsh, N. A. Maleev, S. S. Mikhrin, V. M. Ustinov, A. F. Tsatsul'nikov, M. V. Maximov, B. V. Volovik, D. A. Bedarev, Yu. M. Shernyakov, P. S. Kop'ev, Zh. I. Alferov, N. N. Ledentsov, and D. Bimberg, Appl. Phys. Lett. **75**, 1926 (1999).
[5] V. A. Shchukin, D. Bimberg, V. G. Malyshkin, and N. N. Ledentsov, Phys. Rev. B **57**, 12262 (1998).
[6] X. D. Wang, N. Liu, C. K. Shih, S. Govindaraju, and A. L. Holmes, Jr., Appl. Phys. Lett. **85**, 1356 (2004).
[7] Q. Xie, A. Madhukar, P. Chen, and N. P. Kobayashi, Phys. Rev. Lett. **75**, 2542 (1995).
[8] G. Springholz, V. Holy, M. Pinczolits, and G. Bauer, Science **282**, 734 (1998).
[9] G. Springholz, M. Pinczolits, P. Mayer, V. Holy, G. Bauer, H. H. Kang, and L. Salamanca-Riba, Phys. Rev. Lett. **84**, 4669 (2000).
[10] V. Holy, G. Springholz, M. Pinczolits, and G. Bauer, Phys. Rev. Lett. **83**, 356 (1999).
[11] L. Ouattara, J. M. Ulloa, A. Mikkelsen, E. Lundgren, P. M. Koenraad, M. Borgstrom, L. Samuelson, and W. Seifert, Nanotechnology **18**, 145403 (2007).
[12] M. Gutierrez, M. Herrera, D. Gonzalez, R. Garcia, and M. Hopkinson, Appl. Phys. Lett. **88**, 193118 (2006).
[13] A. J. Koster, R. Grimm, D. Typke, R. Hegerl, A. Stoschek, J. Walz, and W. Baumeister, J. Struct. Biol. **120**, 276 (1997).
[14] R. C. N. Melo, A. M. Dvorak, and P. F. Weller, Microscopy and Analysis **21**, 15 (2007).
[15] H. Friedrich, M. R. McCartney, and P. R. Buseck, Ultramicroscopy **106**, 18 (2005).
[16] P. A. Midgley and M. Weyland, Ultramicroscopy **96**, 413 (2003).
[17] S. Hillyard and J. Silcox, Ultramicroscopy **58**, 6 (1995).
[18] I. Arslan, T. J. V. Yates, N. D. Browning, and P. A. Midgley, Science **309**, 2195 (2005).
[19] T. Inoue, T. Kita, O. Wada, M. Konno, T. Yaguchi, and T. Kamino, Appl. Phys. Lett. **92**, 031902 (2008).
[20] M. Müller, A. Cerezo, G. D. W. Smith, L. Chang, and S. S. A. Gerstl, Appl. Phys. Lett. **92**, 233115 (2008).
[21] J. S. Tsai, J. J. Kai, L. Chang, and F. R. Chen, J. Electron Microsc. **53**, 371 (2004).
[22] A. Nakamura, A. N. Titkov, M. Ichida, V. P. Evtikhiev, and K. Kryganovskii Appl. Phys. A: Mater. Sci. Process. **66**, S1035 (1998).

This article is copyrighted as indicated in the article. Reuse of AIP content is subject to the terms at: http://scitation.aip.org/termsconditions. Downloaded to IP: 140.113.38.11 On: Wed, 30 Apr 2014 22:52:18